



Apparatus to study crystal channeling and volume reflection phenomena at the SPS H8 beamline

Walter Scandale, Ilias Efthymiopoulos, Dean A. Still, Alberto Carnera, Gianantonio Della Mea, Davide De Salvador, Riccardo Milan, Alberto Vomiero, Stefano Baricordi, Stefano Chiozzi, Pietro Dalpiaz, Chiara Damiani, Massimiliano Fiorini, Vincenzo Guidi, Giuliano Martinelli, Andrea Mazzolari, Emiliano Milan, Giovanni Ambrosi, Philipp Azzarello, Roberto Battiston, Bruna Bertucci, William J. Burger, Maria Ionica, Paolo Zuccon, Gianluca Cavoto, Roberta Santacesaria, Paolo Valente, Erik Vallazza, Alexander G. Afonin, Vladimir T. Baranov, Yury A. Chesnokov, Vladilen I. Kotov, Vladimir A. Maishev, Igor A. Yazynin, Sergey V. Afanasiev, Alexander D. Kovalenko, Alexander M. Taratin, Nikolai F. Bondar, Alexander S. Denisov, Yury A. Gavrikov, Yuri M. Ivanov, Vladimir G. Ivochkin, Sergey V. Kosyanenko, Lyubov P. Lapina, Peter M. Levchenko, Anatoli A. Petrunin, Vyacheslav V. Skorobogatov, Vsevolod M. Suvorov, Davide Bolognini, Luca Foggetta, Said Hasan, and Michela Prest

Citation: *Review of Scientific Instruments* **79**, 023303 (2008); doi: 10.1063/1.2832638

View online: <http://dx.doi.org/10.1063/1.2832638>

View Table of Contents: <http://scitation.aip.org/content/aip/journal/rsi/79/2?ver=pdfcov>

Published by the [AIP Publishing](#)

Articles you may be interested in

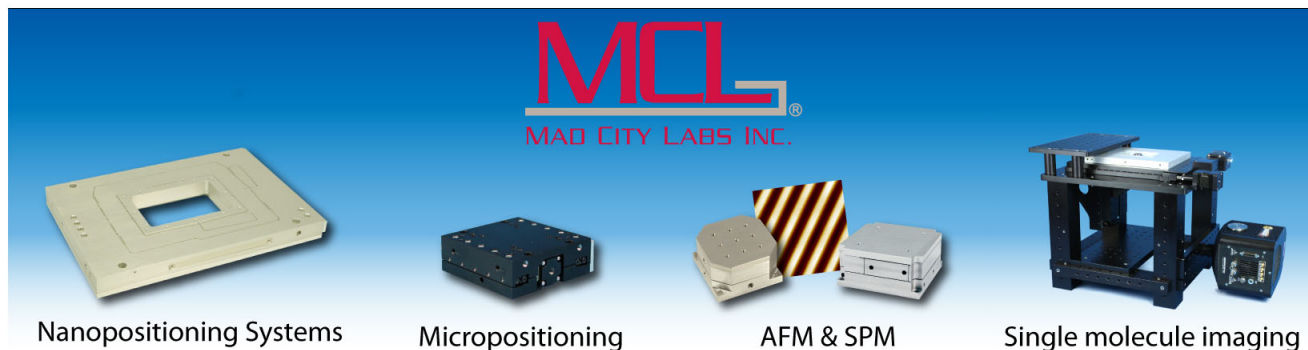
[Low-energy-channeling surface analysis on silicon crystals designed for high-energy-channeling in accelerators](#)
Appl. Phys. Lett. **87**, 094102 (2005); 10.1063/1.2033127

[emiT: An apparatus to test time reversal invariance in polarized neutron decay](#)
Rev. Sci. Instrum. **75**, 5343 (2004); 10.1063/1.1821628

[Virtual instrument automation of ion channeling setup for 1.7 MV tandemron accelerator](#)
Rev. Sci. Instrum. **75**, 4891 (2004); 10.1063/1.1805251

[The EXODET Apparatus And Its First Experimental Results: 17F Scattering By 208Pb Below The Coulomb Barrier](#)
AIP Conf. Proc. **704**, 202 (2004); 10.1063/1.1737112

[Crystal adjustment by means of blocking pattern](#)
Rev. Sci. Instrum. **71**, 2693 (2000); 10.1063/1.1150676



Apparatus to study crystal channeling and volume reflection phenomena at the SPS H8 beamline

Walter Scandale,¹ Ilias Efthymiopoulos,¹ Dean A. Still,² Alberto Carnera,^{3,4} Gianantonio Della Mea,^{3,5} Davide De Salvador,^{3,4} Riccardo Milan,³ Alberto Vomiero,^{3,6} Stefano Baricordi,⁷ Stefano Chiozzi,⁷ Pietro Dalpiaz,⁷ Chiara Damiani,⁷ Massimiliano Fiorini,^{7,a)} Vincenzo Guidi,⁷ Giuliano Martinelli,⁷ Andrea Mazzolari,⁷ Emiliano Milan,⁷ Giovanni Ambrosi,⁸ Philipp Azzarello,⁸ Roberto Battiston,⁸ Bruna Bertucci,⁸ William J. Burger,⁸ Maria Ionica,⁸ Paolo Zuccon,⁸ Gianluca Cavoto,⁹ Roberta Santacesaria,⁹ Paolo Valente,⁹ Erik Vallazza,¹⁰ Alexander G. Afonin,¹¹ Vladimir T. Baranov,¹¹ Yury A. Chesnokov,¹¹ Vladilen I. Kotov,¹¹ Vladimir A. Maishev,¹¹ Igor A. Yazynin,¹¹ Sergey V. Afanasiev,¹² Alexander D. Kovalenko,¹² Alexander M. Taratin,¹² Nikolai F. Bondar,¹³ Alexander S. Denisov,¹³ Yury A. Gavrikov,¹³ Yuri M. Ivanov,¹³ Vladimir G. Ivochkin,¹³ Sergey V. Kosyanenko,¹³ Lyubov P. Lapina,¹³ Peter M. Levchenko,¹³ Anatoli A. Petrunin,¹³ Vyacheslav V. Skorobogatov,¹³ Vsevolod M. Suvorov,¹³ Davide Bolognini,^{14,15} Luca Foggetta,^{14,15} Said Hasan,^{14,15} and Michela Presti^{14,15}

¹CERN, European Organization for Nuclear Research, CH-1211 Geneva 23, Switzerland

²Fermi National Accelerator Laboratory, P.O. Box 500, Batavia, Illinois 60510-0500, USA

³INFN Laboratori Nazionali di Legnaro, Viale Università 2, 35020 Legnaro (PD), Italy

⁴Dipartimento di Fisica, Università di Padova, Via Marzolo 8, 35131 Padova, Italy

⁵Dipartimento di Ingegneria dei Materiali e Tecnologie Industriali, Università di Trento, Via Mesiano 77, 38050 Trento, Italy

⁶INFN-CNR, Via Valotti 9, 25133 Brescia, Italy

⁷INFN Sezione di Ferrara, Dipartimento di Fisica, Università di Ferrara, Via Saragat 1, 44100 Ferrara, Italy

⁸INFN Sezione di Perugia and Università degli Studi di Perugia, Dipartimento di Fisica, Via Pascoli, 06123 Perugia, Italy

⁹INFN Sezione di Roma, Piazzale Aldo Moro 2, 00185 Rome, Italy

¹⁰INFN Sezione di Trieste, Via Valerio 2, 34127 Trieste, Italy

¹¹Institute of High Energy Physics, Moscow Region, RU-142284 Protvino, Russia

¹²Joint Institute for Nuclear Research, Joliot-Curie 6, 141980 Dubna, Moscow Region, Russia

¹³Petersburg Nuclear Physics Institute, 188300 Gatchina, Leningrad Region, Russia

¹⁴Università dell'Insubria, via Valleggio 11, 22100 Como, Italy

¹⁵INFN Sezione di Milano, via Celoria 16, 20133 Milan, Italy

(Received 6 September 2007; accepted 17 December 2007; published online 14 February 2008)

A high performance apparatus has been designed and built by the H8-RD22 collaboration for the study of channeling and volume reflection phenomena in the interaction of 400 GeV/c protons with bent silicon crystals, during the 2006 data taking in the external beamline H8 of the CERN SPS. High-quality silicon short crystals were bent by either anticlastic or quasimosaic effects. Alignment with the highly parallel (8 μ rad divergence) proton beam was guaranteed through a submicroradian goniometric system equipped with both rotational and translational stages. Particle tracking was possible by a series of silicon microstrip detectors with high-resolution and a parallel plate gas chamber, triggered by various scintillating detectors located along the beamline. Experimental observation of volume reflection with 400 GeV/c protons proved true with a deflection angle of (10.4 ± 0.5) μ rad with respect to the unperturbed beam, with a silicon crystal whose (111) planes were parallel to the beam. © 2008 American Institute of Physics. [DOI: 10.1063/1.2832638]

I. INTRODUCTION

Channeling of charged particles in a bent crystal has been envisaged as a useful technique to steer ultrarelativistic beams.¹ Since pioneering experiments² on beam extraction from the Super Proton Synchrotron (SPS), extraction efficiency with crystals has significantly increased with the advent of new solutions for crystal geometries³ and fabrication techniques.^{4,5} As a result, channeling has been investigated in

an increasing number of experiments at accelerators,^{6–10} some of which routinely use bent crystals for beam extraction¹¹ and beam splitting.¹²

A new effect has been recently discovered, which consists in the reversal of the transverse momentum of a charged particle while traversing a bent crystal with a trajectory almost tangent to the crystallographic planes. This effect, traditionally referred to as “volume reflection”, offers new potential for the practical implementation of crystals in accelerators.^{13–15} Thus, interaction of charged particles with a bent crystal appears to be an elegant and efficient technique for manipulation of high energy beams. For example, the use

^{a)}Electronic mail: fiorini@fe.infn.it.

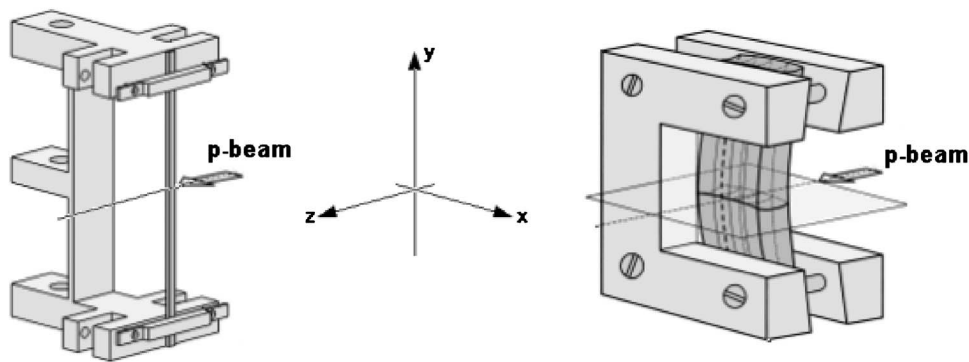


FIG. 1. Schematic drawing of two different types of crystals used in the experiment: a strip (left) and a quasimosaic crystal (right) installed on the corresponding holders which impart the required bending.

of a bent crystal for halo collimation in hadron colliders has already been proposed.¹⁶ Indeed, diffractive physics may take advantage of channeling and volume reflection to increase the acceptance of forward events.¹⁷

The H8-RD22 collaboration aims at a deeper understanding of the interaction of ultrarelativistic protons with bent crystals. The measurement approach relies on precise single-particle tracking¹⁸ with high-resolution silicon microstrip detectors. This article presents a detailed description of the experimental apparatus built and installed in the external line H8 at the CERN SPS and of the technical procedure and preliminary data analysis.

II. SILICON CRYSTALS

Two different types of crystals have been fabricated and used in the experiment: strip and quasimosaic crystals, as schematically shown in Fig. 1.

Silicon strips used in the experiment have been realized at the Sensors and Semiconductors Laboratory at Ferrara University in collaboration with Institute of High Energy Physics (IHEP) (Protvino). Prime materials are the (110) and (111) oriented 4 in. silicon wafers with maximum off-axis orientation of 0.1° , which was the result of a custom-made working process.¹⁹ A wafer with low off-axis orientation is necessary to increase the useful portion of the crystal available for channeling. After standard cleaning procedure, the wafer is diced to achieve the following sizes for the strips, which correspond to the X, Y, and Z coordinates depicted in Fig. 1: $0.2 \times 70 \times 1 \text{ mm}^3$ (ST1 crystal) and $0.5 \times 70 \times 1.85 \text{ mm}^3$ (ST2 crystal), both with the (111) orientation, and $0.9 \times 70 \times 3 \text{ mm}^3$ (ST4 crystal) with the (110) orientation. In order to avoid axial channeling, the dicing is made in such a way that the face exposed to the proton beam is 2° off axis with respect to the crystallographic axis. In order to induce minimal lattice damage, a fine grane blade was used to dice the samples. The residual lattice damage was removed through wet isotropic chemical etching in acids solution (HF, HNO_3 , and CH_3COOH in proportions 2:15:5).⁴ The timing was chosen to remove about $2 \mu\text{m}$. Surface characterization with Rutherford backscattering technique in channeling mode demonstrated the quality of the etched surfaces.²⁰ The crystal is mounted on a specifically designed holder, shown in Fig. 1 (left), which is routinely used at IHEP for beam extraction.¹¹ The holder induces on the crystal a primary curvature and the anticlastic forces give rise to a secondary curvature that is used to deflect the proton beam.

The second type of crystals, in the form of small plates, has been prepared exploiting the elastic quasimosaicity effect, which originates from crystal anisotropy that leads to the curvature of the normal cross sections of the crystal plate under bending.^{21–23} Four silicon plates were prepared in Petersburg Nuclear Physics Institute (PNPI) (Gatchina) in the same way as described in Ref. 5 with the following sizes: $30 \times 58 \times 0.93 \text{ mm}^3$ (QM1 crystal), $30 \times 58 \times 0.84 \text{ mm}^3$ (QM2), $30 \times 58 \times 10 \text{ mm}^3$ (QM3), and $30 \times 30 \times 2.7 \text{ mm}^3$ (QM4). In all the plates, the channeling (111) planes were normal to the large faces and parallel to the long edges. The crystal plates were bent in the YZ plane using a special mechanical device, as shown in Fig. 1 (right) for the case of the simplest device, to induce a quasimosaic curvature of the atomic (111) planes in the XZ plane with a full curvature angle near $100 \mu\text{rad}$. The value of the bending angle was cross-checked with x rays for each crystal. By measuring a rocking curve with x rays, it was found that the thickness of the damaged layer of the plate surfaces is less than $1 \mu\text{m}$. By measuring a diffraction angle from different parts of the crystals, the curvature radius of the large face of the plates in the XZ plane induced by anticlastic forces was found to be $\sim 26 \text{ m}$ and $\sim 100 \text{ m}$ for the QM1 and QM2 crystals, respectively.

III. EXPERIMENTAL LAYOUT

The experiment has been performed in the external line H8 of the SPS accelerator at CERN using a primary proton beam with $400 \text{ GeV}/c$ momentum and very small divergence. The setup, depicted in Fig. 2, consists of a high-precision goniometer (G), used to accurately move the holders with the crystals, a set of high-resolution silicon microstrip detectors placed in the crystal zone (SD0–SD2) and about 70 m downstream (SD3–SD5), a high-rate gas chamber (GC), and a scintillator trigger system (S1–S6, H).

Individual particle trajectories are reconstructed in the silicon microstrip detectors placed upstream and downstream of the goniometer position. The upstream detectors are used to define the particle impact point on the crystal, while the downstream ones, placed at a distance of $65\text{--}74 \text{ m}$, determine the particle deflection with respect to the incident direction. The scintillating detectors define the trigger for the silicon ones and a high rate gas chamber, together with a scintillating hodoscope, is used for fast identification of the channeling conditions.

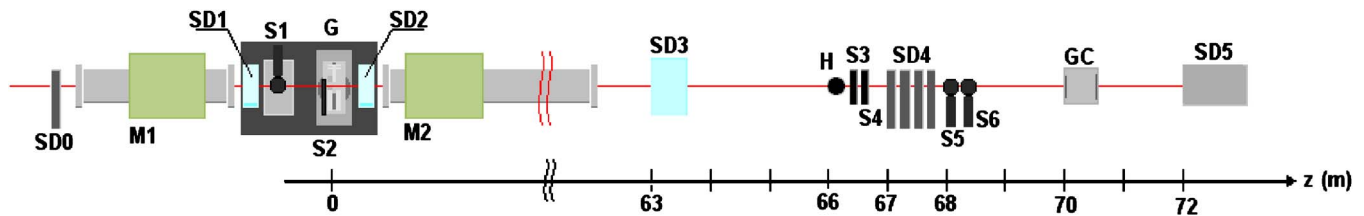


FIG. 2. (Color online) Block diagram of the H8-RD22 experimental setup (not to scale). Not described in the text are M1 and M2, bending magnets already present in the H8 beamline and with no specific function for the experiment.

IV. GONIOMETRIC SYSTEM

The study of channeling phenomena requires very accurate angular alignment of the crystals with respect to the proton beam.

The critical angle for channeling, i.e., the angular acceptance of particle momentum with respect to the crystalline planes, is of the order of $10 \mu\text{rad}$ for 400 GeV/c protons in silicon. Therefore, a high-precision goniometric system was implemented: it consists of two translational stages with $1.5 \mu\text{m}$ accuracy, $2 \mu\text{m}$ bidirectional repeatability, and $5 \mu\text{m}$ resolution over the ranges of 102 mm (upper stage) and 52 mm (lower stage). In between the two translational stages, a rotational one is mounted, with a full range of 360° , $1 \mu\text{rad}$ average accuracy, $1 \mu\text{rad}$ repeatability, and $0.25 \mu\text{rad}$ resolution (the quoted values are the specifications provided by the goniometer producer).

The upper stage is equipped with a platform for simultaneous hosting of two crystal holders; the wide range allows positioning of both crystals on the beam axis. In addition, the range of the lower stage allows positioning the crystals and holders outside the beam. The high accuracy of both translational stages allows micrometric positioning of the crystal with respect to the beam, and an extremely accurate choice of the area of the crystal to be analyzed.

Precise scanning of the channeling peak and accurate measurement of the volume reflection angle requires fine stepping with a resolution better than $3 \mu\text{rad}$. The rotational stage was chosen in order to fulfill all these stringent requirements. The control of angular rotation is provided by an optical encoder and closed loop mechanism, which guarantee the required angular accuracy and repeatability.

All stages are equipped with two-phase microstep motors and mechanical limit switches are integrated in the two linear stages. All the stages are controlled with three axis stand alone controller and power drive. The controller is also equipped with one axis closed loop for the rotational stage with 1 V peak to peak encoder signal, 12 bit resolution.

In order to improve the mechanical stability of the goniometer and to precisely define its relative position with respect to the beam, the whole system was installed on a precisely machined granite table. The goniometer is remotely controlled via a PC and position information is continuously acquired by the data acquisition (DAQ) system of the experiment.

V. PARTICLE TRACKING

The tracking system consists of two types of silicon microstrip detectors having good spatial resolution. These de-

ectors were designed for space-based operation in the AGILE (Ref. 24) and Alpha Magnetic Spectrometer²⁵ (AMS) experiments and are best suited for this experiment in virtue of their resolution and thickness. In particular, AMS-type double sided and AGILE-type single sided silicon microstrip detectors are used in different locations along the beam direction.

Two silicon microstrip stations (AMS and AGILE type) are placed upstream of the goniometer, as shown in Fig. 2, in order to define proton impact point on the crystal surface. The first detector station is of the AGILE type (SD0) and is installed 4.2 m upstream the crystal, while the second is of the AMS type (SD1) and is placed 20 cm upstream the crystal. Another AMS-type silicon detector (SD2) is installed on top of the granite table, 20 cm downstream of the goniometer (G), and defines a point in the proton trajectory after the crystal.

A second set of silicon detectors is placed downstream of the goniometer, in the far detector area, at a distance of 65.0 m for the AMS detectors and 69.1 and 73.9 m for the AGILE ones. The first detector station is composed of four double sided detectors of the AMS type (SD3), mounted at a relative distance of 4 cm. The second station is made of four pairs of single sided silicon microstrip detectors of the AGILE type (SD4), mounted at a relative distance of 21 cm. This station is complemented by a small version of the AGILE tracker called “minitracker” (SD5), with six x - y planes assembled on carbon fiber and aluminum honeycomb trays with a tungsten layer of $300 \mu\text{m}/\text{tray}$, installed 73.9 m downstream the crystal.

The experimental setup includes a fast parallel plate GC and scintillation counters used for triggering and for beam monitoring (S1–S6 and H).

VI. AMS SILICON MICROSTRIP DETECTORS

Silicon detectors stations SD1, SD2, and SD3 are equipped with detector modules of the AMS type.²⁶ These are made of 12 double-sided silicon sensors, $41.360 \times 72.045 \times 0.3 \text{ mm}^3$, grouped together to form a “ladder” with a common bias voltage and readout (Fig. 3).

The n -type, high resistivity sensors are biased with the punch-through technique. p^+ blocking strips, implanted on the n side, are used to minimize the influence of surface charge on the Ohmic side position measurement. The sensors have been designed to exploit interstrip capacitive coupling in order to obtain a very good spatial resolution using a limited number of readout channels. The implantation (readout) strip pitch is $27.5 \mu\text{m}$ ($110 \mu\text{m}$) on the p -side and

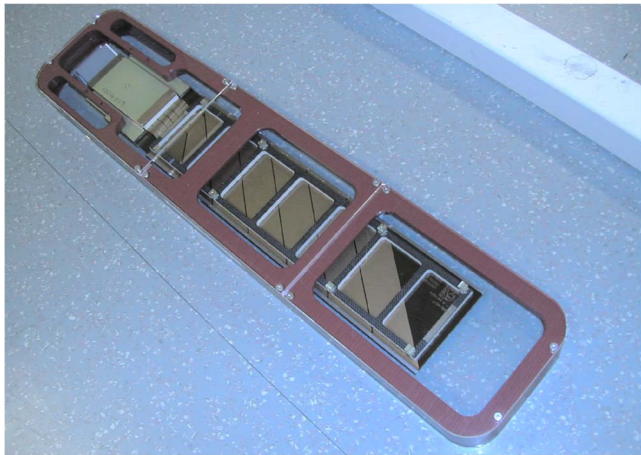


FIG. 3. (Color online) Picture of several 4.1×7.2 cm² AMS double sided silicon sensors, grouped together to form a “ladder” with a common bias voltage and readout.

104 μm (208 μm) on the n side. The finer pitch p -side strips are used to measure coordinate along the bending direction of the beam (X).

The readout strips are ac coupled, via 700 pF capacitor chips, to the VA64.hdr9a, a low noise and high dynamic range front-end chip (IDEAS, Norway). The VA and capacitor chips are located on a standard printed circuit board (hybrid), equipped with ten and six 64-channel chips on the p and n sides, respectively, for a total of 1024 readout channels.

The detector readout is done with the tracker data reduction (TDR) board, a custom board developed for the AMS experiment. Each TDR contains a 12 bit analog-to-digital converter (ADC), a data buffer and a digital signal processor. The latter is programmed to perform on line both the calibration (pedestal and noise calculation) and the zero suppression. A data reduction of about 25 is obtained, allowing operation of the system up to 3 kHz trigger rate without appreciable dead time.

A dedicated beam test to verify the performance of the AMS ladders in terms of spatial resolution has been performed in 2003, yielding a resolution of 8.5 and 30 μm on the p and n sides, respectively. On the H8 beamline, several runs have been devoted to evaluate the alignment parameters of the ladders in the actual configuration and to verify the spatial resolution achieved in this experiment. In Fig. 4, the distribution of track residuals, defined as the distance between the measurements and the fitted track, is presented for tracks reconstructed in the four ladders of the SD3 station. The width of this distribution is related to the measurement error on the single ladder, i.e., the spatial resolution, the uncertainty on the track reconstruction, i.e., the fit error, and possibly to the scattering of the particle along its trajectory. Given the negligible amount of material in the SD3 station, we evaluated the p -side silicon detector resolution for this setup as $\sigma_x = 9.2$ μm , after the fit error subtraction.

VII. AGILE SILICON MICROSTRIP DETECTORS

A second tracking system is based on the AGILE (Ref. 27) silicon sensors (HAMAMATSU, Japan). Each detector is

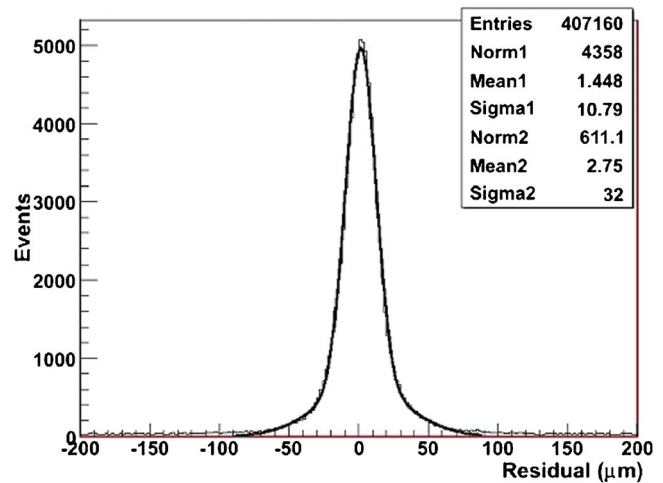


FIG. 4. (Color online) Residual distribution of position measurements for one of the AMS silicon detectors.

a single sided ac coupled 410 μm thick, 9.5×9.5 cm² tile with a physical strip pitch of 121 μm and a readout pitch of 242 μm thus employing a floating strip readout configuration. The detectors have been manufactured on 4 k Ω cm 6 in. wafers, are biased through polysilicon resistors with a voltage lower than 50 V and show a leakage current of less than 1 nA/cm². The detectors are readout by the TAA1 (IDEAS, Norway), an analog digital 128 channel, low noise, self-triggering ASIC. The ASIC is used in a low power configuration (<400 μW /channel) with full analog readout. The TAA1 has been manufactured with BiC metal-oxide semiconductor 0.8 μm technology on epitaxial layer in order to limit latch-up effects. Each channel consists of a folded cascode preamplifier, a CR-RC shaper, a sample-and-hold circuit, and a threshold discriminator with an ASIC global threshold and a 3 bit trim DAC for each channel. The readout is a multiplexed one with a maximum clock rate of 10 MHz. Each tile is readout by three ASICs. The floating strip and the analog information allow to reach a very good spatial resolution keeping power consumption under control.

Figure 5 shows the residuals of one of the AGILE detectors for multistrip clusters. In order to increase the data taking speed, the detectors were readout with the CAEN V550 ADCs in zero suppression mode thus reaching a 1 kHz rate.

VIII. PARALLEL PLATE CHAMBER

A detector for planar channeling studies, capable to withstand high particle rates and working in self-triggering mode, has been developed on the basis of parallel plate gas chamber and successfully used, at first, in the 1 GeV proton channeling experiment at PNPI.¹⁴ In the H8 data taking this detector is used for fast angular scanning of crystals, to get information on their orientation with respect to the beam and to provide online characterization of the crystals under investigation.

The detector consists of two parallel flat electrodes assembled with a uniform gap and installed within an aluminum frame of 25(height) \times 110(width) \times 175(length) mm³, filled with a gas mixture (70% Ar+30% CO₂) at atmospheric pressure. The anode electrode is arranged on a glass-ceramic

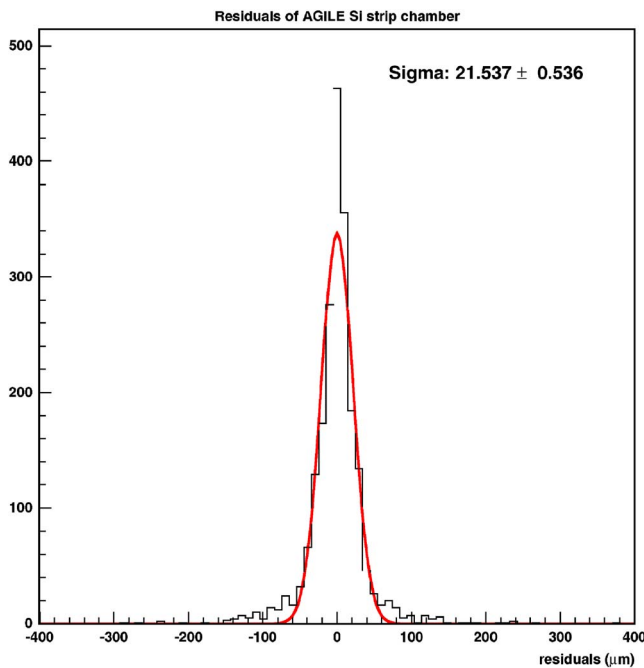


FIG. 5. (Color online) Residual distribution of position measurements for the AGILE detectors.

plate covered by Ni–Cu–V multilayer and treated photolithographically to produce 64 strips, 150 μm wide, with a 200 μm pitch. The cathode electrode is made from low-resistance sputtered silicon plate of $0.5 \times 10 \times 50 \text{ mm}^3$. The silicon plate is glued on the anode through insulator spacers providing a 600 μm distance between electrodes. Thus, the working volume of the detector is restricted to a dimension of $0.6(\text{height}) \times 12.8(\text{width}) \times 10(\text{length along the beam}) \text{ mm}^3$. The frame of the detector is equipped with two capton windows for the proton beam, inlet and outlet for the gas mixture, and electrical connectors for high voltage supply and signals read out from the strips.

The front-end electronics of the detector consists in an individual amplifier shaper and discriminator for each strip arranged on the four AD16_F boards²⁸ developed originally for amplifying and discriminating the anode signals of the proportional chambers of the end-cap muon system of the Compact Muon Solenoid (CMS) detector. In working conditions, the amplifier noise is typically 1 fC and the thresholds of all discriminators are set close to the minimum value of 7 fC.

The working position of the detector corresponds to the particles passing through the gap parallel to the electrodes and anode strips. Such geometry enables to increase the working volume to detect particles up to 10 mm (size of anode electrode) but makes the chamber gain dependent on the distance between the particle track and the anode. The largest signals are formed by particles traveling near the cathode, while the smallest are formed by particles near the anode. A threshold of the front-end electronics determines the fraction of the chamber gap where incident protons are detected. The straggling of thresholds in channels results in the straggling of sensitive volumes corresponding to different strips. In practice, this straggling is taken into account by

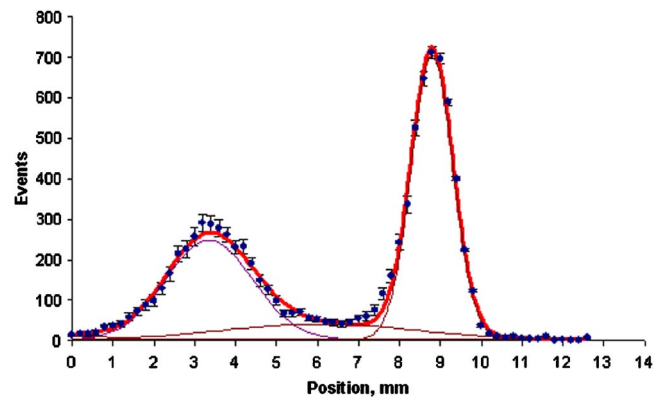


FIG. 6. (Color online) Beam profile measured with the parallel plate chamber and QM3 crystal in channeling position (x is mm, y is events). Results of the fit with three Gaussians describing channeled (right peak), nonchanneled (left peak) and dechanneled (area between peaks) fractions are also presented on the plot ($\chi^2/\text{ndf}=2.11$).

means of a calibration procedure. For a uniform parallel beam, the efficiency of the chamber can be defined as the ratio of the detected particles to all the particles crossing the gap. From measurements with 1 GeV protons, the efficiency is found to be 20% and corresponds to the detection of protons within 1/5 of the gap near the cathode with a probability close to 1.

Due to the relatively small active area, the detector was mounted on a moving support, with a stepping precision of 4 μm and a total range of about 50 mm for both horizontal and vertical movements. This provided the initial positioning of the detector on the beam axis. One of the beam profiles measured using the gas chamber with QM3 crystal in the channeling position is shown in Fig. 6.

IX. SCINTILLATORS AND TRIGGER SYSTEM

Two thin scintillation counters were installed on the granite table (S1, 100 μm thick in the bending plane) and on the upper linear stage of the goniometer (S2, 80 μm thick). They were used to define the exact beam position with respect to the crystals. A pair of identical scintillators (S3–S4: $100 \times 100 \times 4 \text{ mm}^3$) was placed downstream of the AMS ladders (SD3) and used to define the trigger for the silicon detectors. Two additional scintillators were used in the downstream detector region: a 100 μm thick (S5) and a 2 mm thick one (S6), mounted on moving supports for a redundant measurement of the beam divergence and profile.

A scintillating hodoscope (H), made of 16 vertical strips with a total sensitive area of $3.2 \times 4.0 \text{ cm}^2$, was used for beam monitoring. Each strip is $2(\text{horizontal}) \times 4(\text{along beam}) \times 40(\text{vertical}) \text{ mm}^3$, slightly overlapping with the neighboring ones in order to avoid dead space. The strips are read out by a 16 channel photomultiplier (Hamamatsu H6568), which enables to have fast signals and low cross-talk. The hodoscope was used during data taking to provide fast information on crystal alignment and beam stability.

Scintillator electronics is composed of commercial modules based on Nuclear Instrumentation Module (NIM) and Versa Module Europa (VME) standards. The signals are sent

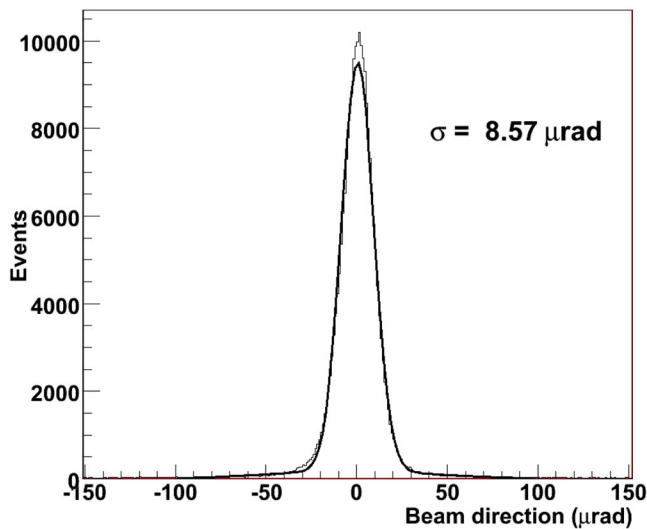


FIG. 7. (Color online) Residuals of the downstream AMS detector, with respect to the upstream one, from which a beam divergence of $(7.84 \pm 0.07) \mu\text{rad}$ can be extracted (see text for details).

to a programmable trigger logic unit, a custom module which generates the trigger signals for the silicon microstrip detectors, receiving as input the discriminated signals from all the scintillators and the hodoscope, in addition to busy signals from silicon stations and the SPS accelerator signals.

X. PROTON BEAM

The H8 external beamline is located in the North Area of the CERN SPS. The experiment used a 400 GeV/c primary proton beam with an intensity of about 2×10^{12} ppp, which was reduced to about 5×10^4 ppp. The beam had a continuous time structure with a flat top of 4.8 s duration every 16.8 s.

The beam spot diameter at the crystal has been measured with silicon microstrip detectors to be about 1 mm. The beam divergence has been measured, in dedicated runs without crystal, from the angular distribution of beam particles reconstructed with the upstream (SD1) and downstream (SD3) stations. In Fig. 7, the reconstructed angular distribution of particles is shown: it is peaked around the nominal beam direction and the spread ($8.57 \mu\text{rad}$) reflects the beam divergence and its widening due to multiple scattering on the material between SD1 and SD3 along the beamline. With a dedicated GEANT4 Monte Carlo simulation, the multiple scattering contribution has been estimated to be $(3.46 \pm 0.03) \mu\text{rad}$. Subtracting in quadrature this contribution yields a beam divergence at the crystal of $(7.84 \pm 0.07) \mu\text{rad}$.

XI. EXPERIMENTAL PROCEDURE

After installation of the holders with crystals on top of the goniometer, an optical prealignment was performed using a laser beam. The laser ray, parallel to the beam axis, was sent perpendicularly to the crystal surface with the help of a pentaprism. Being the path of the laser beam of about 10 m

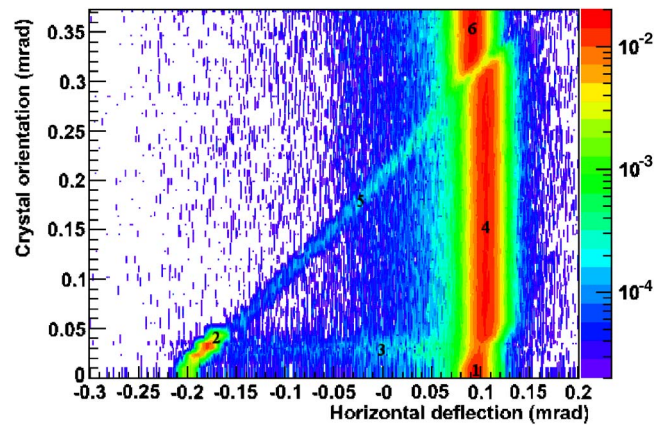


FIG. 8. (Color online) Beam intensity as a function of the crystal orientation angle (vertical axis) and of the measured beam deflection (horizontal axis) for ST1 strip crystal. The channeling peak (2) and the large volume reflection region (4) are clearly visible.

and the precision on the measured position of the reflected ray of 1 mm, crystal prealignment with the beam was possible with an accuracy of about 0.1 mrad.

After laser prealignment, a fast scan of the crystal angular position has been performed measuring proton tracks with the parallel plate chamber, thanks to the high particle rate it can sustain. A $10\text{--}20 \mu\text{rad}$ rotation of the crystal was performed every accelerator cycle and the corresponding beam profile was recorded 70 m downstream of the goniometer. This measurement defined, precisely and in a short time, the channeling angular position and the total angular range to be measured with higher statistics and higher precision using the silicon detectors.

A more detailed scan was then performed with angular steps of $3\text{--}5 \mu\text{rad}$, recording silicon detectors data for about $10\text{--}15$ accelerator cycles for each crystal position, in order to collect enough statistics for offline data analysis. A custom made client/server protocol, based on TCP/IP and python, allowed for the communication between the main data acquisition computer (MDAQ), and the various subsystems of the experiment: the goniometer control system, the trigger control system, and the silicon detectors DAQ systems. The MDAQ was able to move the goniometer and to start and stop the data acquisition runs, allowing for automatic data taking at different crystal orientations. Typically about 150 and 45 K events were collected in the AMS and AGILE detectors for each goniometer position.

The result of such angular scan for the ST1 strip crystal is presented in Fig. 8, which shows the normalized beam intensity as a function of the angle of the crystalline planes with respect to the beam (vertical axis) and of the angular deflection of the particles measured 65 m downstream of the crystal with silicon microstrip detectors (horizontal axis).

Region (1) in Fig. 8 pertains the beam traversing the crystal in a nonaligned orientation: no deflection is observed. Increasing the goniometer angle, the channeling condition is met, i.e., most of the particles are captured in the crystalline planes and steered outward, resulting in the peak (2) clearly visible in the bottom-left part of the plot. The channeling peak is separated from the unperturbed beam by

(278.2 ± 3.2) μrad , which corresponds to the crystal bending angle (measured with optical techniques) within experimental errors. A small fraction of the initially channeled particles exits the channel due to an increase of the transverse energy (dechanneled particles) and is visible in region (3).

The volume reflection region appears when the goniometer angle is further increased: the particle enters the crystal with a too high transverse energy for being channeled at the surface. At some place inside the crystal, the particle trajectory becomes almost tangent to the bent crystalline planes and here two phenomena may occur. The particle may lose a fraction of its transverse energy and be trapped in the potential well: the particle is channeled within the volume of the crystal (volume capture) and the resulting distribution is visible in region (5). As an alternative, the transverse momentum of the particle may be reversed as in the scattering off a potential barrier (volume reflection). The volume reflection region (4) extends over a wide angular area along the vertical axis: almost the whole beam is displaced by (10.4 ± 0.5) μrad with respect to the unperturbed beam, in the opposite direction to that of channeling. In region (6) volume reflection is no longer possible and the crystal is traversed by the incoming particles in a nonoriented condition, similar to region (1).

Offline analysis show a channeling efficiency of (38.5 ± 2.7)% and a volume reflection efficiency which amounts to (98.3 ± 0.5)%. The last figure of merit highlights good perspectives for manipulation of a proton beam via interactions with a bent crystal in volume reflection mode.

XII. CONCLUSIONS

An experimental setup for precise measurement of channeling and volume reflection phenomena in the interaction of charged particles with bent crystals has been designed and built. The key features of the system are an ultraprecise goniometer and a high-resolution tracking system.

The experimental setup has been successfully used to study, with very high accuracy, channeling, and volume reflection phenomena of protons in new generation silicon crystals during a dedicated data taking in the SPS H8 beamline. During the two week data taking period, more than a thousand runs have been recorded to disk and, in total, three strip crystals and two quasisosaic crystals were fully characterized. First results have already been published,¹⁵ more detailed data analysis will be the subject of another publication.

ACKNOWLEDGMENTS

We gratefully acknowledge support from L. Gagnon, P. Lebrun, S. Myers, Alexei A. Vorobyev, Victor A. Gordeev, Alexei N. Sissakian, Alexander I. Malakhov, Nikolai E. Tyurin, A. Sambo, E. Boscolo Marchi, A. Papi, V. Postolache, and G. Alberti. We also acknowledge partial support by the European Community-Research Infrastructure Activity under the FP6 "Structuring the European Research Area" program (CARE, Contract No. RII3-CT-2003-506395), the INTAS program, the INFN NTA-HCCC and MIUR 2006028442 Projects, Russian Foundation for Basic Re-

search Grant No. 06-02-16912, Council of the President of the Russian Federation Grant No. NSh-3057.2006.2, "Physics of Elementary Particles and Fundamental Nuclear Physics" Program of the Russian Academy of Sciences.

- ¹E. Tsyganov, Fermilab International Report No. TM-682, 1976.
- ²H. Akbari, X. Altuna, S. Bardin, R. Bellazzini, V. Biryukov, A. Brez, M. P. Bussa, L. Busso, A. Calcaterra, G. Carboni, F. Costantini, R. De Sangro, K. Elsener, F. Ferioli, A. Ferrari, G. P. Ferri, F. Ferroni, G. Fidecaro, A. Freund, R. Guinand, M. Gyr, W. Herr, A. Hilaire, B. N. Jensen, J. Klem, L. Lanceri, K. Maier, M. M. Massai, V. Mertens, S. P. Møller, S. Morganti, O. Palamara, S. Péraire, S. Petrerá, M. Placidi, R. Santacesaria, W. Scandale, R. Schmidt, A. M. Taratin, F. Tosello, E. Uggerhøj, B. Vettermann, P. F. Vita, G. Vuagnin, E. Weisse, and S. Weisz, *Phys. Lett. B* **313**, 491 (1993).
- ³A. G. Afonin, V. T. Baranov, V. M. Biryukov, M. B. H. Breese, V. N. Chepegin, Yu. A. Chesnokov, V. Guidi, Yu. M. Ivanov, V. I. Kotov, G. Martinelli, W. Scandale, M. Stefanchik, V. I. Terekhov, D. Trbojevic, E. F. Troyanov, and D. Vincenzi, *Phys. Rev. Lett.* **87**, 094802 (2001).
- ⁴V. M. Biryukov, Yu. A. Chesnokov, V. Guidi, V. I. Kotov, C. Malagù, G. Martinelli, W. Scandale, M. Stefanchik, and D. Vincenzi, *Rev. Sci. Instrum.* **73**, 3170 (2002).
- ⁵Yu. M. Ivanov, A. A. Petrunin, and V. V. Skorobogatov, *JETP Lett.* **81**, 99 (2005).
- ⁶A. G. Afonin, V. T. Baranov, V. M. Biryukov, V. I. Kotov, V. A. Maisheev, V. I. Terekhov, E. F. Troyanov, Yu. S. Fedotov, V. N. Chepegin, Yu. A. Chesnokov, Yu. M. Ivanov, V. Guidi, G. Martinelli, M. Stefanchik, D. Vincenzi, D. Trboevich, V. Scandale, and M. B. H. Breese, *JETP Lett.* **74**, 55 (2001).
- ⁷S. P. Møller, E. Uggerhøj, H. W. Atherton, M. Clément, N. Doble, K. Elsener, L. Gagnon, P. Grafström, M. Hage-Ali, and P. Siffert, *Phys. Lett. B* **256**, 91 (1991).
- ⁸R. A. Carrigan, Jr., D. Chen, G. Jackson, N. Mokhov, C. T. Murphy, S. Baker, A. Bogacz, D. Cline, S. Ramachandran, J. Rhoades, J. Rosenzweig, A. Asseev, V. Biryukov, A. Taratin, J. A. Ellison, A. Khanzadeev, T. Prokofieva, V. Samsonov, G. Solodov, B. Newberger, E. Tsyganov, H.-J. Shih, W. Gabella, B. Cox, V. Golovatyuk, and A. McManus, *Phys. Rev. ST Accel. Beams* **5**, 043501 (2002).
- ⁹R. P. Filler, III, A. Drees, D. Gassner, L. Hammons, G. McIntyre, S. Peggs, D. Trbojevic, V. Biryukov, Y. Chesnokov, and V. Terekhov, *Phys. Rev. ST Accel. Beams* **9**, 013501 (2006).
- ¹⁰S. Stokov, T. Takahashi, I. Endo, M. Inuma, K. Ueda, H. Kuroiwa, T. Ohnishi, and S. Sawada, *Nucl. Instrum. Methods Phys. Res. B* **252**, 16 (2006).
- ¹¹A. G. Afonin, V. M. Biryukov, V. A. Gavrilushkin, V. N. Gres, B. A. Zelenov, V. I. Kotov, V. A. Maisheev, A. V. Minchenko, V. N. Terekhov, E. F. Troyanov, Yu. A. Chesnokov, M. G. Gordeeva, A. S. Denisov, Yu. M. Ivanov, A. A. Petrunin, V. V. Skorobogatov, and B. A. Chudin, *JETP Lett.* **67**, 781 (1998).
- ¹²C. Biino, N. Doble, L. Gagnon, P. Grafstrom, and H. Wahl, *Proceedings of the European Particle Accelerator Conference, 1998* (unpublished), pp. 2100-2102.
- ¹³Yu. M. Ivanov, A. A. Petrunin, V. V. Skorobogatov, Yu. A. Gavrikov, A. V. Gelamkov, L. P. Lapina, A. I. Schetkovsky, S. A. Vavilov, V. I. Baranov, Yu. A. Chesnokov, A. G. Afonin, V. T. Baranov, V. N. Chepegin, V. Guidi, W. Scandale, and A. Vomiero, *Phys. Rev. Lett.* **97**, 144801 (2006).
- ¹⁴Yu. M. Ivanov, N. F. Bondar, Yu. A. Gavrikov, A. S. Denisov, A. V. Zhelamkov, V. G. Ivochkin, S. V. Kos'yanenko, L. P. Lapina, A. A. Petrunin, V. V. Skorobogatov, V. M. Suvorov, A. I. Shchetkovsky, A. M. Taratin, and W. Scandale, *JETP Lett.* **84**, 372 (2006).
- ¹⁵W. Scandale, D. A. Still, A. Carnera, G. Della Mea, D. De Salvador, R. Milan, A. Vomiero, S. Baricordi, P. Dalpiaz, M. Fiorini, V. Guidi, G. Martinelli, A. Mazzolari, E. Milan, G. Ambrosi, P. Zazarello, R. Battiston, B. Bertucci, W. J. Burger, M. Ionica, P. Zuccon, G. Cavoto, R. Santacesaria, P. Valente, E. Vallazza, A. G. Afonin, V. T. Baranov, Y. A. Chesnokov, V. I. Kotov, V. A. Maisheev, I. A. Yaznin, S. V. Afansiev, A. D. Kovalenko, A. M. Taratin, A. S. Denisov, Y. A. Gavrikov, Y. M. Ivanov, V. G. Ivochkin, S. V. Kosyanenko, A. A. Petrunin, V. V. Skorobogatov, V. M. Suvorov, D. Bolognini, L. Foggetta, S. Hasan, and M. Prest, *Phys. Rev. Lett.* **98**, 154801 (2007).
- ¹⁶V. M. Biryukov, V. N. Chepegin, Y. A. Chesnokov, V. Guidi, and W. Scandale, *Nucl. Instrum. Methods Phys. Res. B* **234**, 23 (2005).
- ¹⁷CARE HHH Workshop Proceedings, 2007 (unpublished).

- ¹⁸M. Fiorini, G. Ambrosi, R. Assmann, C. Biino, Y. Chesnokov, P. Dalpiaz, I. Efthymiopoulos, L. Gatignon, V. Guidi, Y. Ivanov, R. Santacesaria, W. Scandale, A. Taratin, and A. Vomiero, Proceedings of the European Particle Accelerator Conference, 2006 (unpublished), pp. 1538–1540.
- ¹⁹V. Guidi, A. Antonini, S. Baricordi, F. Logallo, C. Malagù, E. Milan, A. Ronzoni, M. Stefancich, G. Martinelli, and A. Vomiero, Nucl. Instrum. Methods Phys. Res. B **234**, 40 (2005).
- ²⁰S. Baricordi, V. M. Biryukov, A. Carnera, Yu. A. Chesnokov, G. Della Mea, V. Guidi, Yu. M. Ivanov, G. Martinelli, E. Milan, S. Restello, A. Sambo, W. Scandale, and A. Vomiero, Appl. Phys. Lett. **87**, 094102 (2005).
- ²¹O. I. Sumbaev, Zh. Eksp. Teor. Fiz. **54**, 1352 (1968) [Sov. Phys. JETP **27**, 724 (1968)].
- ²²V. M. Samsonov, Leningrad Institute of Nuclear Physics, USSR Academy of Sciences, LIYaF AN SSSR Report No. 278, 1976.
- ²³V. M. Samsonov and E. G. Lapin, Leningrad Institute of Nuclear Physics, USSR Academy of Sciences, Report No. 587, LIYaF AN SSSR, 1980.
- ²⁴F. Longo, A. Argan, N. Auricchio, G. Barbiellini, A. Bulgarelli, P. Caraveo, E. Celesti, A. Chen, V. Cocco, E. Costa, G. Di Cocco, G. Fedel, M. Feroci, M. Fiorini, T. Froyland, M. Galli, F. Gianotti, A. Giuliani, C. Labanti, I. Lapshov, F. Lazzarotto, P. Lipari, A. Mauri, M. Marisaldi, S. Mereghetti, E. Morelli, A. Morselli, L. Pacciani, F. Paladin, A. Pellizzoni, F. Perotti, P. Picozza, C. Pittori, C. Pontoni, J. Porrovecchio, B. Preger, M. Prest, M. Rapisarda, E. Rossi, A. Rubini, P. Soffitta, M. Tavani, A. Traci, M. Trifoglio, E. Vallazza, S. Vercellone, and D. Zanello, Nucl. Phys. B, Proc. Suppl. **125**, 222 (2003).
- ²⁵M. Aguilar *et al.*, Phys. Rep. **366**, 331. (2002).
- ²⁶J. Alcaraz *et al.*, Il Nuovo Cimento **112A**, 1325 (1999).
- ²⁷G. Barbiellini, G. Fedel, F. Liello, F. Longo, C. Pontoni, M. Prest, M. Tavani, and E. Vallazza, Nucl. Instrum. Methods Phys. Res. A **490**, 146 (2002).
- ²⁸http://hepd.pnpi.spb.ru/hepd/red/products/Front_End_en.html